Viscosity of methane to 6 GPa and 673 K

Evan H. Abramson[*]

Department of Earth and Space Sciences, University of Washington, Seattle 98195, Washington, USA
(Received 6 October 2011; revised manuscript received 5 December 2011; published 30 December 2011)

A rolling-sphere technique has been used to measure shear viscosities of (supercritical) fluid methane in a diamond-anvil cell between temperatures of 294 and 673 K, up to a pressure of 6 GPa. A correlation between a reduced viscosity and reduced residual entropy is shown to give a good account of much of the extant data, both from this study and the literature.

Introduction. As part of a program to determine the shear viscosities of small molecules at high densities, I present here measurements taken on methane for temperatures between 294 and 673 K and up to the melting pressures. Methane is a subject of both experimental and theoretical interest; a sizeable body of data already exists at low and intermediate pressures as summarized in [1]. Data have also been taken up to 1 GPa at 273 K [2] and at 298 K [3], and to 0.08 GPa and a maximum temperature of 523 K [4]. Given its nature as a psuedospherical molecule, it was interesting to see whether methane would continue to behave akin to a hard sphere or, at higher densities, exhibit a "locking" of rotational motion as surmised in Refs. [2,3].

Experiment. The technique has been described in several previous publications [5–7]. High pressures were generated with diamond-anvil cells of a modified Merrill-Basset design, using anvils with ~650 μm diameter culets and gaskets of hardened Inconel 718. Both ruby [8] and Sm-doped SrB_4O_7 [9] were used to measure pressure with a typical precision of 0.02 GPa. The cell was loaded by immersion in cryogenic liquid methane condensed from the gas (nominal purity 99.995%). The cell was placed in an oven and temperature was measured to an accuracy of 1 K with chromel-alumel thermocouples located in proximity to the diamonds.

In addition to the pressure marker, each of the loads contained a single platinum sphere of ~40 μm diameter. The cell and its enclosing oven were located on a combined tilt-rotation stage which allowed the plane of the diamond culets to be inclined with respect to the horizontal, typically between 15 and 30°, and the cell then to be rotated about the normal to the plane until the sphere was toward the top. As the sphere rolled down the plane of the lower diamond, its trajectory was recorded with a video camera (100 frames/s). Plots of the speed against the sine of the angle of inclination formed straight lines, the slopes of which were inversely proportional to the viscosity of the surrounding fluid. For any sphere the constant of proportionality could be determined by filling the cell with a fluid of known viscosity, in these experiments either toluene at 1 bar [10] or water at 0.1 GPa [11].

Results. Measurements were taken on approximate isotherms of 294, 373, 473, 573 and 673 K; results (Table I) are

plotted in Fig. 1. The viscosities, η, are well represented by the equation [6]

$$\ln(\eta) = \ln\{\eta_{\mathrm{dilute}}\rho_0/[(B-1)\rho + \rho_0]\} + B\rho/(\rho_0 - \rho), \quad (1)$$

where ρ is the density, η_{dilute} is the viscosity of the dilute gas [1] at the given temperature, and B and ρ_0 are constants for each isotherm. A simultaneous fit to all the data (curves through data in Fig. 1) with $B = 6.71 + 1.969 \times 10^{-2}T$ and ρ_0 (g cm^{-3}) $= 0.799 + 4.055 \times 10^{-3}T$ provides a root-mean-square misfit of 1.8%. Throughout this paper derived thermodynamic quantities (density and entropy) are taken from [12] in which the equation of state is described by an expansion of the Helmholtz energy in terms of density and (inverse) temperature, and other quantities are obtained by the appropriate combination of derivatives. Taking into account random uncertainties of the individual measurements in methane (the fractional uncertainty of the slope, δ, for each least-squares fit of rolling speed is given in Table I) and also in the calibration of the various spheres, the absolute error of the overall fit to Eq. (1) is believed to be better than 4% over the range of the data.

Figure 2 shows deviations from the fit for pressures below 1.5 GPa, where current data may be compared with previously obtained values. Equation (1) typically underestimates viscosities along lower-temperature isotherms at lower pressures, with the maximum error occurring at about the critical density (for methane, roughly 0.03 GPa at 298 K). The general form of the deviations in Fig. 2 is thus expected, the maximum being comparable to that for carbon dioxide [13] while somewhat larger than for argon [14] and significantly larger than for nitrogen [15], presumably reflecting the progression toward smaller attractive forces in the series.

The correlation between a reduced viscosity, η_{red}, and reduced residual entropy, s, noted [13–15] in other systems holds also for methane as shown in Fig. 3. The variables of the plot are

$$\eta_{\mathrm{red}} = \eta \rho_{\mathrm{melt}}^{-2/3}(mkT)^{-1/2} \text{ and } \quad s = -(S - S_{\mathrm{ideal}})/Nk, \quad (2)$$

where ρ_{melt} is the particle density of the fluid at its melting pressure (at the relevant temperature [16]), m is the particle mass, k is Boltzmann's constant, and S is the entropy, while S_{ideal} is the entropy the fluid would have if it were an ideal gas at the same density and temperature. Note that in Rosenfeld's

————————
[*]evan@ess.washington.edu

TABLE I. Measured pressures, temperatures, viscosities and nominal fractional uncertainties (1σ) of viscosities, with densities and reduced residual entropies from [12].

P (GPa)	T (K)	η (mPa s)	δ (%)	ρ (g cm^{-3})	s
0.57	295.0	0.202	3	0.5089	3.42
0.85	294.3	0.303	4	0.5520	3.90
1.07	294.5	0.422	2	0.5781	4.20
1.15	294.7	0.472	4	0.5866	4.29
1.16	294.5	0.463	5	0.5876	4.31
1.20	294.8	0.484	3	0.5916	4.35
1.26	293.2	0.522	4	0.5979	4.44
1.32	294.5	0.568	2	0.6032	4.49
1.49	372.7	0.419	1	0.6016	4.08
1.43	473.7	0.294	3	0.5771	3.49
3.22	475.8	0.844	1	0.6965	4.62
1.56	576.3	0.257	3	0.5721	3.20
2.76	578.0	0.502	3	0.6578	3.92
3.08	574.5	0.574	2	0.6759	4.09
3.52	575.6	0.678	2	0.6979	4.28
4.17	575.2	0.901	3	0.7272	4.54
4.32	574.6	0.909	4	0.7335	4.60
2.69	676.8	0.419	2	0.6411	3.55
4.61	674.5	0.817	2	0.7340	4.31
4.90	674.8	0.864	4	0.7453	4.40
5.75	676.8	1.082	4	0.7757	4.65
6.26	684.7	1.199	5	0.7918	4.76

FIG. 2. (Color online) Measured viscosities at lower pressures are plotted up to 1.5 GPa as fractional deviations from the fit to Eq. (1). Error bars are estimates of 1σ values. Data from van der Gulik *et al.* (vdG, Refs. [2,3]) are also shown. In order to maintain the clarity of the plot, data from Golubev [4] (taken up to 0.08 GPa) were not included; it can be seen below in Fig. 4 that these data tend to lie at lower values than reported in Refs. [2,3] for the same temperatures.

original proposal [17] viscosity was reduced by the fluid density at the relevant temperature and pressure; since this causes a divergence as density tends to zero I use here an altered definition in which a reasonable defining distance is taken to be proportional to the cube root of the (liquid) molecular volume at the melting point, that is, the closest one may pack the molecules at any particular temperature before
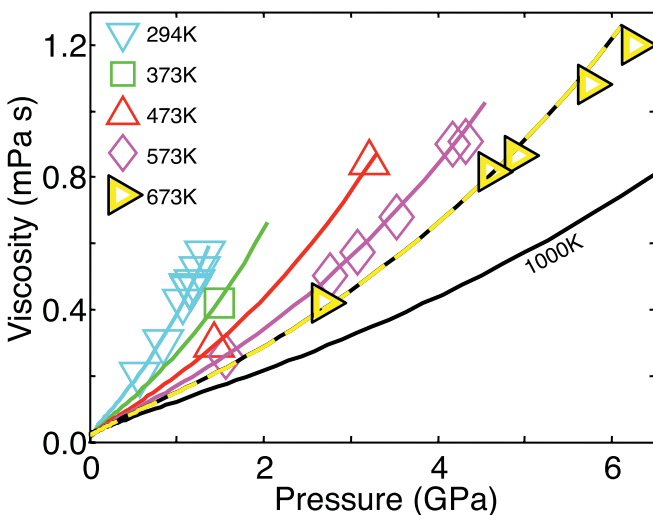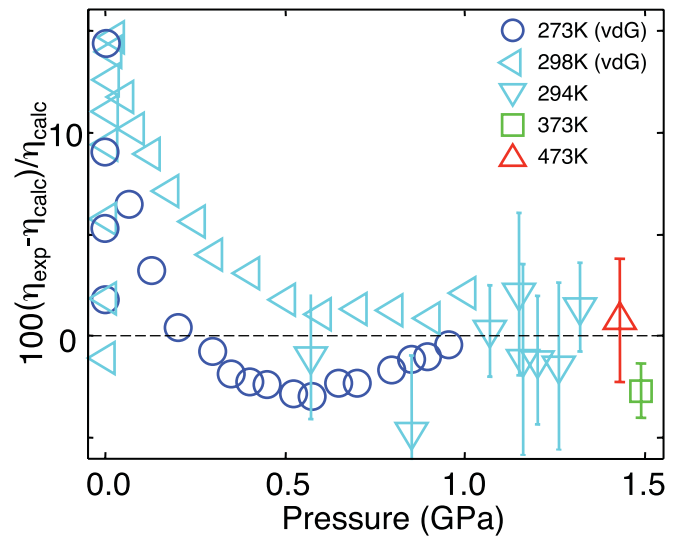

FIG. 1. (Color online) Measured viscosities are plotted against pressure along several isotherms. Curves representing the lowest five isotherms are calculated from the fit to Eq. (1). The predicted 1000 K isotherm is derived from the straight, dashed line in Fig. 3.
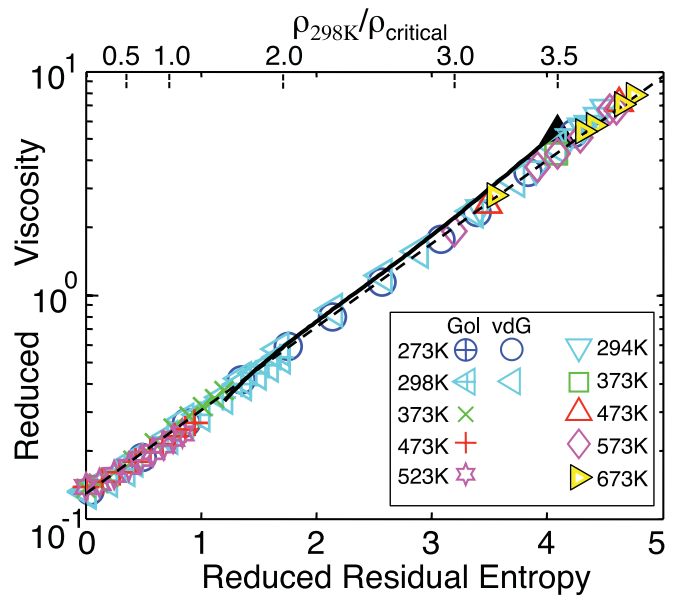

FIG. 3. (Color online) Reduced viscosity is plotted against reduced residual entropy [Eqs. (2)]. The solid curve represents values (as calculated from Ref. [1]) along the line of vapor-liquid equilibrium [12] from (1 K below) the critical point to the triple point (solid triangle). Data from van der Gulik *et al.* (vdG, Refs. [2,3]) and from Golubev (Gol, Ref. [4]) are included. The scale at the top pertains to a 298 K isotherm and gives the ratio of fluid density to that at the critical point. Densities range from that of the 1 bar gas ($s = 0$) to a factor of 4.9 times the critical value. The straight, dashed line drawn through the data is used to calculate the 1000 K isotherm in Fig. 1 and the deviations in Fig. 4.
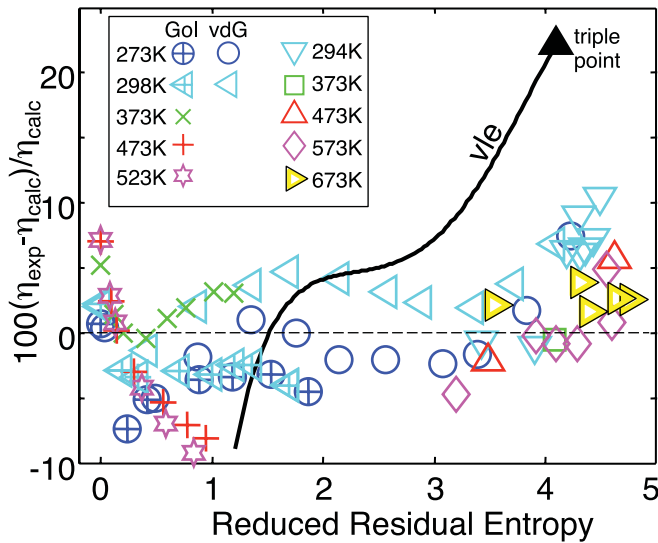
FIG. 4. (Color online) Measured viscosities are plotted as fractional deviations from the straight, dashed line in Fig. 3. Data from van der Gulik *et al.* (vdG, Refs. [2,3]) and from Golubev (Gol, Refs. [4]) are included. The solid curve represents values (as calculated from Ref. [1]) along the line of vapor-liquid equilibrium [12], from (1 K below) the critical point to the triple point.
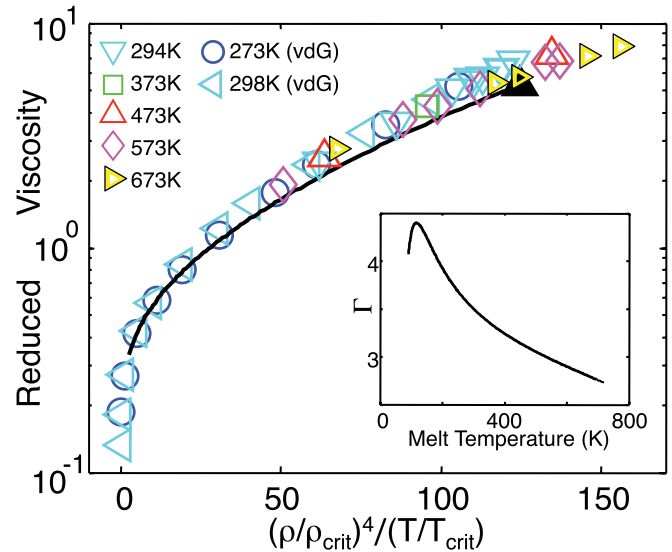

FIG. 5. (Color online) Reduced viscosity [Eqs. (2)] is plotted against the quantity $(\rho/\rho_{\rm crit})^4/(T/T_{\rm crit})$, here normalized to the value at the critical point. Symbols are the same as in previous figures. The inset contains values of Γ (computed from Refs. [12,16]) plotted against the melting temperature.

the solid becomes the stable phase. The figure contains current experimental results along with viscosities previously reported for the supercritical fluid between 0 and 1 GPa, and in the subcritical liquid. The scale at the top indicates the ratio of the density to the critical density for the 298 K isotherm. At the highest pressure in the study (and 684 K) the density is a factor of 4.9 larger than the critical density.

The data of Fig. 3 may be approximated by a straight line in the semilogarithmic plot, $\ln(\eta_{\rm red}) = 0.860s - 2.05$. Deviations from this fit are shown in Fig. 4. Uncertainty in entropy can account for some of the deviation, especially when extrapolating the equation of state to pressures in excess of 1 GPa. However, the 1% uncertainty estimated [12] for specific heats, integrated between the triple point and 298 K, leads to an error of only ~0.07 e.u. and is unlikely to be the source for the large departure of the subcritical liquid as it approaches the triple point. The correlation does yield an excellent account of the higher temperature data and, insofar as the entropy is adequately known, is expected to be a better predictor of viscosities in extrapolation than Eq. (1). It seems likely therefore that the large deviations to lower viscosities of the 473 and 523 K points of Ref. [4] is indicative of systematic error in those experiments; this view is corroborated by comparison of the 273 and 298 K data of Ref. [4] with those of Refs. [2,3]. Viscosities at higher pressures and temperatures may be predicted by calculating for each point a value of s, then using the line in Fig. 3 to define a value of $\eta_{\rm red}$ and thence η. In Fig. 1 a curve of predicted viscosities at 1000 K is drawn in this manner.

Fragiadakis and Roland [18] have shown that fluids of small, nonassociating molecules have kinetic properties which, when suitably reduced, scale to the quantity T/ρ^γ with γ a constant of the system; further, for molecules approximating

hard spheres γ is found to have a value equal to the thermodynamic quantity $\Gamma = d \ln(T_{\rm melt})/d \ln(\rho_{\rm melt})$. One of the systems considered was methane, which at lower pressures was found to have viscosities and, separately, melting densities scaling as $\gamma \approx \Gamma \approx 4$. Figure 5 demonstrates that for reduced viscosities the utility of this scaling persists up to the pressures and temperatures of the current study. Again, viscosities along the line of vapor-liquid equilibrium are seen to depart from the higher-temperature data; a somewhat tighter correlation of the latter can be achieved with $\gamma = 3.9$, but only at the cost of increasing deviation along the vapor-liquid line. The interesting equation noted in [18] between γ and Γ does not hold at higher pressures and temperatures. Indeed, Γ is not constant over the larger range of this extended data set; as seen in the inset to Fig. 5, it decreases from a maximum of 4.4 at 120 K down to a value of 2.8 for the 673 K melt.

Van der Gulik *et al.* [2,3] suggested that at the highest pressures of their experiments (0.8–1.0 GPa) and close to the melting point, the viscosities increased with pressure more rapidly than expected, possibly due to a locking of rotational motion. The current data, while not as precise as the former, do indicate a continuation of the trend noted in the 298 K study. Still, at a comparable temperature (294 K) the maximum density in this study is 6% higher than in the previous, while the present 684 K data extend to a value 39% higher. It seems likely that such a large increase in what was already a liquid-like packing of molecules would have caused a fluid on the verge of rotational locking to demonstrate a radical divergence in viscosity, even at the larger temperature.

[1] D. G. Friend, J. F. Ely, and H. Ingham, J. Phys. Chem. Ref. Data **18**, 583 (1989).

[2] P. S. van der Gulik, R. Mostert, and H. R. van den Berg, Fluid Phase Equilib. **79**, 301 (1992).

[3] P. S. van der Gulik, R. Mostert, and H. R. van den Berg, Physica A (Amsterdam) **151**, 153 (1988).

[4] I. F. Golubev, *Viscosity of Gases and Gas Mixtures (A Handbook)* (Israel Program for Scientific Translations, Jerusalem, 1970), p. 83.

[5] H. E. King Jr., E. Herbolzheimer, and R. L. Cook, J. Appl. Phys. **71**, 2071 (1992).

[6] E. H. Abramson, J. Chem. Phys. **122**, 084501 (2005).

[7] E. H. Abramson, Phys. Rev. E **76**, 051203 (2007).

[8] H. K. Mao, J. Xu, and P. M. Bell, J. Geophys. Res. **91**, 4673 (1986).

[9] E. H. Abramson and J. M. Brown, Geochim. Cosmochim. Acta **68**, 1827 (2004).

[10] C. L. Yaws, *Handbook of Transport Property Data: Viscosity, Thermal Conductivity, and Diffusion Coefficients of Liquids and Gases* (Gulf Pub. Co., Houston, 1995), p. 43.

[11] R. A. Perkins, A. Laesecke, D. G. Friend, J. V. Sengers, M. J. Assael, I. N. Metaxa, E. Vogel, R. Mares, and K. Miyagawa, J. Phys. Chem. Ref. Data **38**, 101 (2009).

[12] U. Setzmann and W. Wagner, J. Phys. Chem. Ref. Data **20**, 1061 (1991).

[13] E. H. Abramson, Phys. Rev. E **80**, 021201 (2009).

[14] E. H. Abramson, High Pressure Res. **31**, 544 (2011).

[15] E. H. Abramson and H. West-Foyle, Phys. Rev. E **77**, 041202 (2008).

[16] E. H. Abramson, High Pressure Res. **31**, 549 (2011).

[17] Y. Rosenfeld, Phys. Rev. A **15**, 2545 (1977).

[18] D. Fragiadakis and C. M. Roland, Phys Rev. E **83**, 031504 (2011).